ELSEVIER

PII: S0032-3861(98)00013-5

Polymer Vol. 39 No. 18, pp. 4349–4358, 1998

0032-3861/98/$19.00+0.00

Structure and properties of polyaniline films prepared via electrochemical polymerization. I: Effect of pH in electrochemical polymerization media on the primary structure and acid dissociation constant of product polyaniline films

Hikaru Okamoto* and Tadao Kotaka
Graduate School of Engineering, Toyota Technological Institute, 2-12-1 Hisakata, Tempaku, Nagoya 468, Japan
(Received 27 June 1997; revised 12 September 1997; accepted 17 December 1997)

Electrochemical polymerization of aniline was conducted in *constant current* mode at different pH ranging from 0.2 to 3.7 in an ITO glass electrode–quartz cell assembly for in situ monitoring of the changes in potential, amount of charge passed through, and u.v.–visible absorption (u.v.–Vis) spectra during polymerization. u.v.–Vis spectra of product polyaniline (PAn) films were determined in different pH solutions to evaluate the apparent acid dissociation constants $(pKa)_{app}$ from plots of $\log\{(Abs_{HAX} - Abs_{obs})/(Abs_{obs} - Abs_A)$ *versus* pH, where Abs_{obs}, Abs_{HAX}, and Abs_A are the observed absorption strength and those of the fully protonated and deprotonated species, respectively, for a given wavelength light. In PAn films prepared at low pH (< 1.0), *emeraldine* form PAn chains with relatively long average conjugation length but broad distribution were produced, while in those prepared at high pH (> 1.5), PAn chains with short conjugation length were produced and later deteriorated as the polymerization proceeded, because the polymerization potential eventually exceeded a critical value ($+ 0.8$ V) beyond which degradation of produced PAn chains took place.

(Keywords: polyaniline; electrochemical polymerization; effect of pH)

INTRODUCTION

Conducting polymers such as polyaniline, polypyrrole and polythiophene have been paid much attention as key materials for developing electronic devices, e.g., Li batteries[1,2], capacitors, and other electrochromic devices[3,4]. Such applications utilize to the best advantage their features in doping/dedoping reactions, reversible changes in conductivity and/or absorption spectra upon potential switching. To obtain a high-performance conductive polymer film it is essential to fabricate the polymer into a thin film of fine and well-defined structure preferably with a large surface area, which makes its response faster and more effective.

Among these conductive polymers, polyaniline (PAn) appears to be promising because of its good stability in air and of the ease in preparing a thin film via electrochemical polymerization[5]. However, the details of the reaction are still not very well understood. Indeed, the reaction mechanisms are complicated, as compared with other conducting polymers, presumably because the polymerization of PAn includes not only redox reaction but also protonation/deprotonation to nitrogen atoms in aniline moieties[6–8]. Thus the polymerization conditions, especially, pH of the solution may affect the reaction, resulting in PAn chains of different primary structure which leads to a film of different gross morphology with different structural size[9,10].

Versatility in the primary structure is presumably a result of the difference in the protonation behaviour of aniline in the polymerization mixture and the PAn chains growing on the electrode. In the course of the electrochemical polymerization, nucleation takes place on the fresh surface of the electrode. Then growth of PAn chains on the nuclei follows and the deposited PAn chains play the role of newly formed surface for the further polymerization. The characteristics of the formed PAn film, e.g. the acid dissociation constant (p*K*a) and conductivity, may thus dominate the further reaction. In fact, we observed different u.v.–visible absorption spectra and different p*K*a values for PAn films polymerized in solutions of different pH. These results may reflect differences in the primary structures of the PAn chains in the film such as having 'head-to-tail' junctions *versus* 'head-to-head' and/or 'tail-to-tail' heterojunctions[11,12]. The different spectra may also reflect differences in the higher-order structures or morphologies in the PAn films.

There are a few studies on nucleation and growth in the electrochemical polymerization of aniline[13,14]. In such studies they interpreted the features of transient electrolysis current by applying a theory of metal deposition in electroplating[15–17]. However, in the electrochemical polymerization of aniline, the electrode surface continuously changes its characteristics as the electrolysis proceeds, as opposed to the electroplating process in which always a fresh surface of the same characteristics is created. Thus for understanding of the electrochemical polymerization process, it is indispensable to examine the structural development of PAn films throughout the whole course of polymerization.

* To whom correspondence should be addressed

In this series of studies we have attempted to follow, by use of specially designed cell systems, the whole process of structural development of PAn films under different acidity conditions, and employing in situ techniques of time-resolved u.v.–visible (u.v.–Vis) spectroscopy and chronoamperometry/potentiometry (CA/CP). After the polymerization, the PAn films were subjected to out-of-situ characterization via cyclic voltammetry (CV) combined with u.v.–Vis spectroscopy. Changes in absorption spectra upon pH change were also examined to evaluate apparent acid dissociation constants $(pKa)_{app}$ of the films prepared under different conditions. Herein we will report the results.

EXPERIMENTAL

Preparation of polyaniline (PAn) films

For the electrochemical polymerization of aniline the monomer, aniline (Wako Pure Chemicals, Co.), was first purified by distillation under reduced pressure of 3 torr and the fraction distilling between 44 to 45°C was collected. Solutions containing 0.1 M (mol L^{-1}) aniline were prepared and their pH was adjusted by adding HCl and/or KCl from pH = − 0.5 to 4.5 but keeping chloride ion concentration constant: $[Cl^-]$ = 1 M (mol L^{-1}). The pH was measured with a pH meter (D-13; Horiba Seisakusho, Kyoto) for the range of pH > 0, while for pH < 0 it was estimated from the amount of HCl added to the solution by employing reported activity values[18].

The electrochemical polymerization was conducted at 25°C via a *constant current* (*galvanostatic*) mode with a current density of 40 μA cm^{-2} (unless otherwise specified) on an indium–tin oxide (ITO) glass electrode in a specially designed electrolysis cell. The current was controlled with a potentio-galvanostat (HA-301, Hokuto Denko) with a function-generator (HB-104; Hokuto Denko) and the electrolysis potential was monitored simultaneously. In a few trial runs of polymerization, we employed a *constant potential* (*potentiostatic*) mode with + 0.75 V at pH = 0.2 just to compare the performance of the constant current mode to the constant potential mode.

The polymerization cell was a 1 × 1 cm^2 quartz cell mounted on a u.v.–visible absorption spectrometer (UV-160A; Shimadzu Seisakusho, Ltd) to monitor time development of absorption spectra. As is illustrated in *Figure 1*, the cell was equipped with a working electrode (WE) made of ITO-glass (Evers Co., Ltd), a platinum-wire counter electrode (CE) and a miniature Ag/Ag^+/3 M NaCl electrode (RE-4; BAS) used as a reference electrode (RE). We used ITO glasses with 200 to 205 nm thickness ITO layer deposited on soda glass, which were obtained from a single batch, annealed in air at 360°C for 10 min to condition their surfaces. Transparency of the ITO-electrode was more than 82% for 550 nm light and its sheet resistance was in the range 8–10 Ω cm^{-2}. The Pt wire used as the CE was placed at a location against the WE where the electrolysis current became homogeneous as much as possible. With these u.v.–Vis and CA/CP monitoring systems, we followed electrolysis potential between the WE and RE, the amount of charge passed through, and u.v.–Vis spectra during the polymerization.

On several occasions, we also monitored changes of electric impedance of deposited PAn films. The measurement was carried out with an LCR meter (HP2484A; Hewlett–Packard) mounted in the polymerization cell system. For AC current measurement with the LCR meter, another Pt wire electrode was placed close to the WE in the cell. Impedance at 10 kHz between the WE and the Pt wire electrode was monitored and in-phase component (Z'), out-of-phase component (Z'') and the absolute value $|Z| = \sqrt{(z')^2 + (z'')^2}$ of the impedance were evaluated. The observed impedance involved extra contributions from electric double layer and ionic conduction in the solution, which we did not separate from the contribution of the PAn film.

Cyclic voltammetry with the simultaneous monitoring of absorption strength

Some preliminary runs indicated that a prolonged polymerization under the constant current mode yielded an extremely poor quality film, which often peeled off from the electrode, releasing filmy fragments in the solution. Thus after passing 0.04 to 0.06 C cm^{-2} charge (1000 to 1500 s), we stopped the electrolysis and took out the WE with deposited PAn film, rinsed it several times in alkali and pure water, and then subjected it to cyclic voltammetry (CV) with absorption strength monitoring. The CV measurements were carried out at 25°C on the solution containing almost the same constituents, less the aniline, as were used for the polymerization. The applied potential was swept from − 0.2 V to + 0.8 V and reversed to − 0.2 V at a rate of 10 mV s^{-1}.

FTi.r. spectroscopy

To confirm whether unusual chemical bonds had been created in PAn chains we subjected PAn films recovered at the end of the polymerization under different conditions to *FT*i.r. spectroscopy. The PAn films prepared at different pH were torn from the ITO electrode and mixed with KBr to form pellets. The *FT*i.r. measurement (FT-730; Horiba) was carried out between 4000 and 400 cm^{-1} with 10-fold integration.

u.v.–Vis spectra in media of different pH but at the same counter ion concentration

First we examined spectral changes of PAn films upon pH change in adequately buffered media. For comparison, aniline monomer and related dimers, *N*-phenyl-*p*-phenylenediamine ('head-to-tail' dimer) and hydrazobenzene ('head-to-head' dimer) were also examined. In each test a rinsed PAn film was immersed in a 0.1 M KH_2PO_4 buffer solution with its pH being adjusted to a value between 13 and 0 by titrating it with HCl or KOH plus KCl to keep $[Cl^-]$

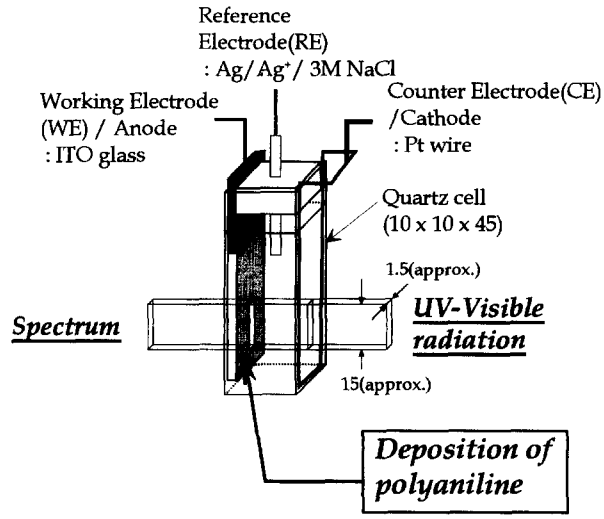

Figure 1 Configuration of an electrochemical u.v.–Vis spectrometry cell used in this study

= 1 M, and the u.v.–Vis spectra were observed again at 25°C in media of different pH. On the other hand, aniline monomer and the two dimers were dissolved directly in the same buffer solution, and their spectral changes were observed.

Evaluation of apparent acid dissociation constants

For a PAn film we define the *apparent* acid dissociation constant $(pKa)_{app}$ from absorption strength data obtained from a film prepared by varying the pH. First, we assume equilibrium protonation of an aniline moiety in a PAn chain as:

$$[=(C_6H_4)=N^+(H)(X^-)-] \rightleftarrows [=(C_6H_4)=N-]+H^+ +X^- \quad (1)$$

which is abbreviated as:

$$H^+A(X^-) \rightleftarrows A+H^+ +X^-$$

An aniline moiety in the PAn chain acquires a proton H^+ together with a dopant anion X^- to neutralize itself and releases the proton plus the anion to establish the protonation/deprotonation equilibrium. Thus the concentration of dopant counter-anions $[X^-]$ affects the equilibrium. Then the acid dissociation constant Ka can be defined for the equilibrium given by equation (1) as:

$$Ka=\frac{[H^+][A(X^-)]}{[H^+A(X^-)]} \quad (2a)$$

$$pKa=pH-\log\frac{[A]}{[H^+A(X^-)]}-\log[X^-] \quad (2b)$$

The concentrations of the species of $A(X^-)$ and $H^+A(X^-)$ are dependent on $[X^-]$. Then from the observed absorption strength (Abs_{obs}) at a given pH and those of fully protonated (Abs_{HAX}) and unprotonated (Abs_A) species for the light of an adequately chosen wavelength at which the dynamic range of the absorption strength is the largest, we assume:

$$\frac{[A]}{[H^+A(X^-)]}=\frac{(Abs_{HAX}-Abs_{obs})}{(Abs_{obs}-Abs_A)} \quad (3a)$$

Now combining equations (2) and (3), we define the *apparent* acid-dissociation constant $(pKa)_{app}$ as

$$(pKa)_{app}=pH-\log\frac{(Abs_{HAX}-Abs_{obs})}{(Abs_{obs}-Abs_A)}-\log[X^-] \quad (3b)$$

Thus, we can define '*effective* acid dissociation constant (p*Ka**)' as the pH where [A] = [HAX], or more precisely, where Abs_{obs} reaches a half of the total change ($Abs_{HAX} - Abs_A$), i.e., $(Abs_{HAX} - Abs_{obs}) = (Abs_{obs} - Abs_A)$:

$$pKa^* = (pKa)_{app}+\log[X^-] \quad (3c)$$

Then, if $[X^-]$ is 1 M and $\log[X^-] = 0$, $pKa^* = (pKa)_{app}$, 'the *apparent* acid dissociation constant', which is, for a *single-species two-state* system such as aniline, equivalent to the true acid dissociation constant, if the counter-anion concentration or the ionic strength of the medium is specified.

RESULTS

Effect of pH on electrochemical polymerization behaviour

Figure 2 compares time developments of u.v.–Vis spectra with polymerization time t collected at 2 min intervals up to 24 min for the solutions at four different pH. Here we notice that the shape of the spectra and the development with t are strongly dependent on the pH of the solution. At low pH (< 1) the spectral shape remains essentially the same but with its intensity increasing with t. The peak wavelength gradually shifts to the longer wavelength side owing partly to the gradual decrease in the potential, as seen in *Figure 3*(b), under the *constant-current* mode polymerization. On the other hand, in those at higher pH (> 1) the spectra look quite different with the broad peaks around 600 and 750 nm shifting gradually toward the shorter wavelength side.

Figure 3(a) shows changes of the absorption strength monitored at 800 nm wavelength, which reflects the amount of PAn deposited on the electrode (monomer-to-polymer conversion), against t or the amount of total charge in coulombs (C) passed through the cell. *Figure 3*(b)*Figure 3*(c), respectively, show changes in the electrolysis potential and in the complex impedance, Z', Z'' and $|Z|$, with t for PAn films deposited on the WE at pH 0.2 and 3.7.

In the runs at low pH, the peak intensity increases roughly linearly with time, while the electrolysis potential is high for a brief period in the very beginning, rapidly drops and

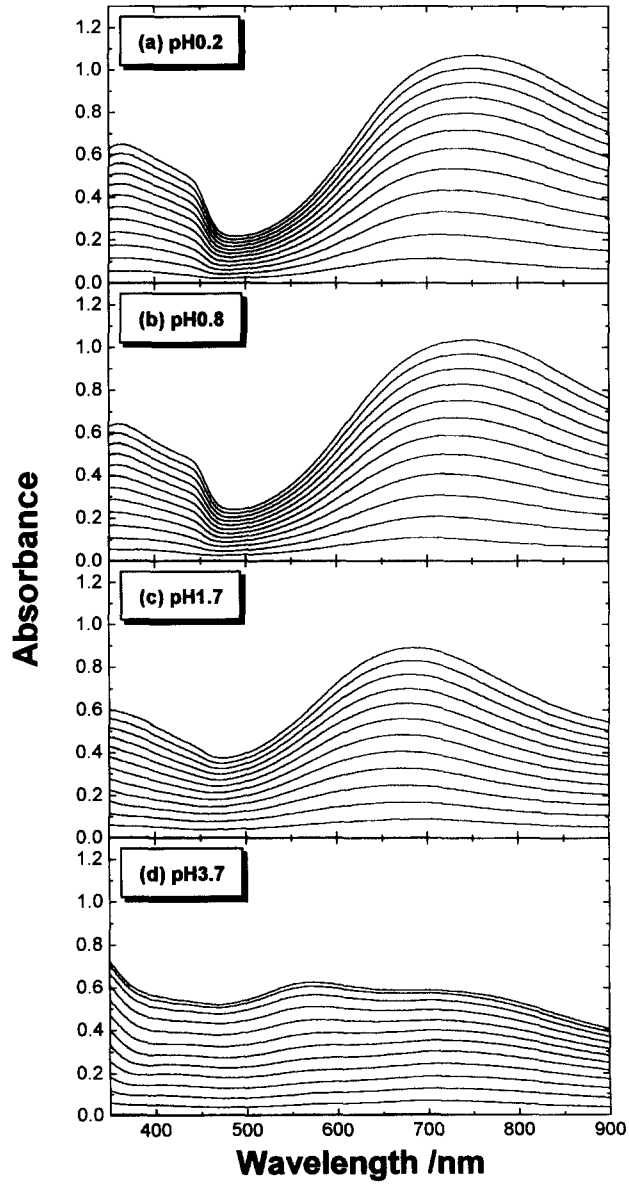

Figure 2 Time development of u.v.–Vis spectra of polyaniline films at two-minute intervals up to 1440 s during electrochemical polymerization in *constant current* mode with 40 $\mu A\ cm^{-2}$ at different pH: (a) 0.2; (b) 0.8; (c) 1.7; (d) 3.7

afterwards remains nearly constant at a certain level below + 0.8 V. The change in $|Z|$ with t at pH 0.2 is quite similar to that of the potential and it consists almost exclusively of Z' with little Z'' except in the very early stage. However, in the runs at high pH (> 2), the absorption strength develops rather slowly and tends to level off after a certain polymerization time, implying depolymerization of the formed chains might be taking place. On the other hand, the electrolysis potential starts from a low level but eventually begins to increase steadily and exceeds the level of + 0.8 V, which appears to be a critical value for the chain breaking to take place. Impedance data collected at pH 3.7 exhibit a rapid increase especially beyond this + 0.8 V limit, accompanying a rapid increase in the contribution of Z'' component. This result implies the deposition of non-conductive PAn chains upon WE forming a condenser.

Cyclic voltammograms of PAn films polymerized at different pH

After passing 0.04 to 0.06 C cm^{-2} current, we stopped the polymerization and made simultaneous observation of the CV and absorption strength at 420 nm of the resulting PAn films in 1 M HCl solution by sweeping the potential from − 0.2 to + 0.8 V and back at a rate of 10 mV s^{-1}. *Figure 4* shows the results.

Figure 4(a), *Figure 4*(b) show the results for PAn films polymerized at pH = 0.2 and 0.8, respectively. The voltammograms look similar to those reported in the literature[5,9,11]. In these voltammograms, we see two pairs of anodic and cathodic peaks at almost the same positions: one is a pair of strong peaks at about + 0.25 V and + 0.1 V corresponding to the redox reaction of PAn itself, and the other is a pair of weak peaks appearing at about + 0.55 V and + 0.45 V corresponding presumably to the redox reaction of a degradation product, which was suggested to

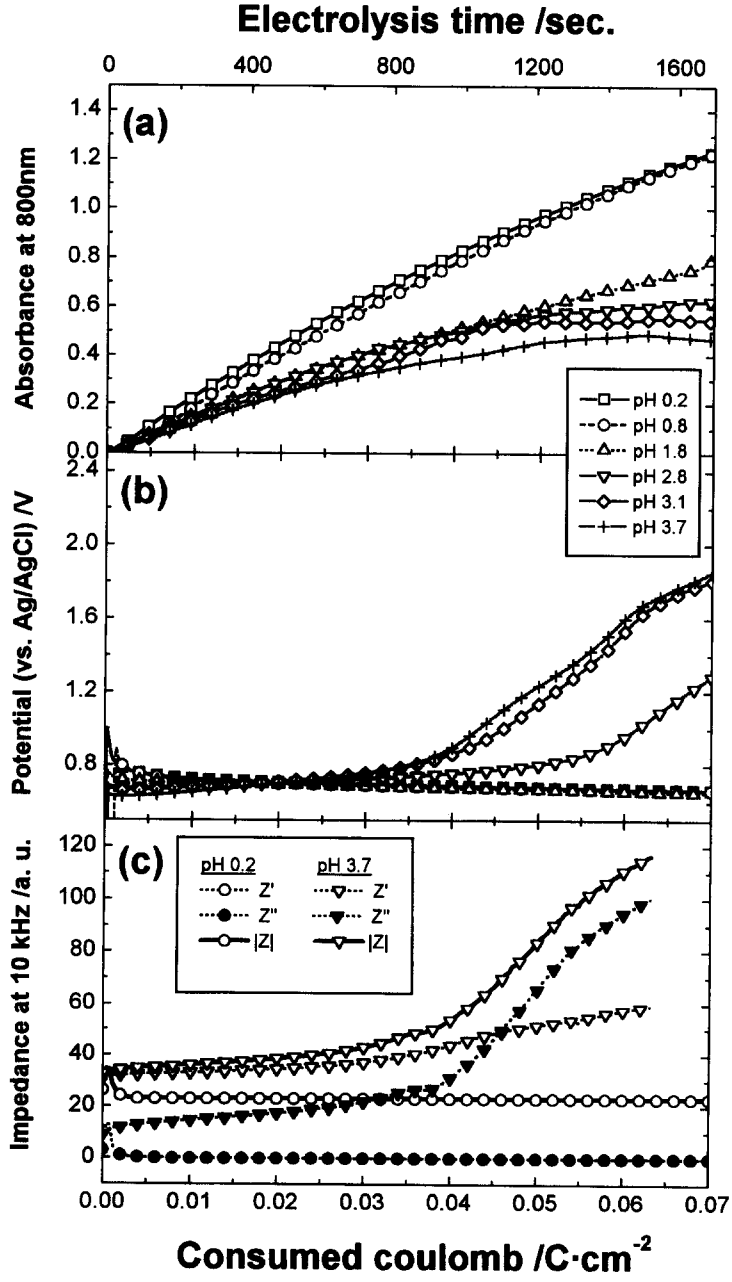

Figure 3 Changes of (a) absorption strength for 800 nm light, (b) applied potential and (c) impedance against polymerization time (or consumed coulombs) during *constant current* electrolysis with 40 $\mu A\ cm^{-2}$ in solutions of different pH

be *p*-benzoquinone[11,19,20]. The absorbance *versus* potential curves show hysteresis in the range between about + 0.3 V and − 0.2 V. The hysteresis is sometimes called 'memory effect' or 'slow relaxation'[21,22] that reflects difference in the rates of redox reaction and/or protonation/deprotonation reactions.

On the other hand, *Figure 4*(c), *Figure 4*(d) show the results for PAn films polymerized at pH = 1.7 and 3.7. We see especially in the latter the main anodic and cathodic peaks are shifted to + 0.4 and + 0.25 V, while the subpeaks remain the same as those of the other films but with the strength becoming much stronger. For the PAn film prepared at pH = 3.7, the absorbance *versus* potential curve shows extremely strong hysteresis: The going and returning curves are entirely different in shape and even the loop does not close. This means that the electrochemical reactions at this high pH are irreversible.

*FT*i.r. spectra

The u.v.–Vis spectra and CV voltammograms presented above suggest that the primary structure is entirely different for PAn chains prepared at low and high pH: Possibly *p*-benzoquinone type heterolinkages[11,19,20] might exist in the PAn film polymerized at high pH (> 3.7). In fact, Ohsaka et al.[24] previously conducted electrochemical polymerization of aniline in aqueous solutions at pH = 1 and 7 as well as in acetonitrile solution. They reported that those obtained in the latter two cases yielded quite unusual i.r. spectra, strongly suggesting the formation of unusual linkages. We thus attempted to identify these by comparing the *FT*i.r. spectra of the films obtained at pH = 0.2, 1.7 and 3.7 to see whether or not such unusual linkages might have been created. In particular, we looked for unusual IR peaks around 1655 cm^{-1} range attributable to C=O groups of *p*-benzoquinone[20,25].

Examples of the *FT*i.r. spectra are shown in *Figure 5*. We see that, as already reported in the literature[20,24,25], all the PAn films give nearly identical spectra with the peaks corresponding to the signals such as ν(N–H), ν(C–C), ν(C–N) and γ(C–H)expected for *para*-substituted 'head-to-tail' bonds in the PAn backbones. The spectra obtained are quite similar to that reported by Ohsaka et al. for PAn obtained at pH = 1[24]. The two peaks seen at 1300 and 1250 cm^{-1} were attributed by Ohsaka et al.[24] to stretching vibration of C–N bonds of secondary aromatic amines, and the single peak at 820 cm^{-1} to out-of-plane bending vibration of C–H bonds of *para*-substituted aromatic ring[24].

Concerning heterojunctions or unusual chemical bonds, Ohsaka et al.[24] reported that a PAn film obtained at pH = 7 exhibited a peak at 1450 cm^{-1} corresponding to stretching vibration of N–N bonds, two other strong peaks at 850 and

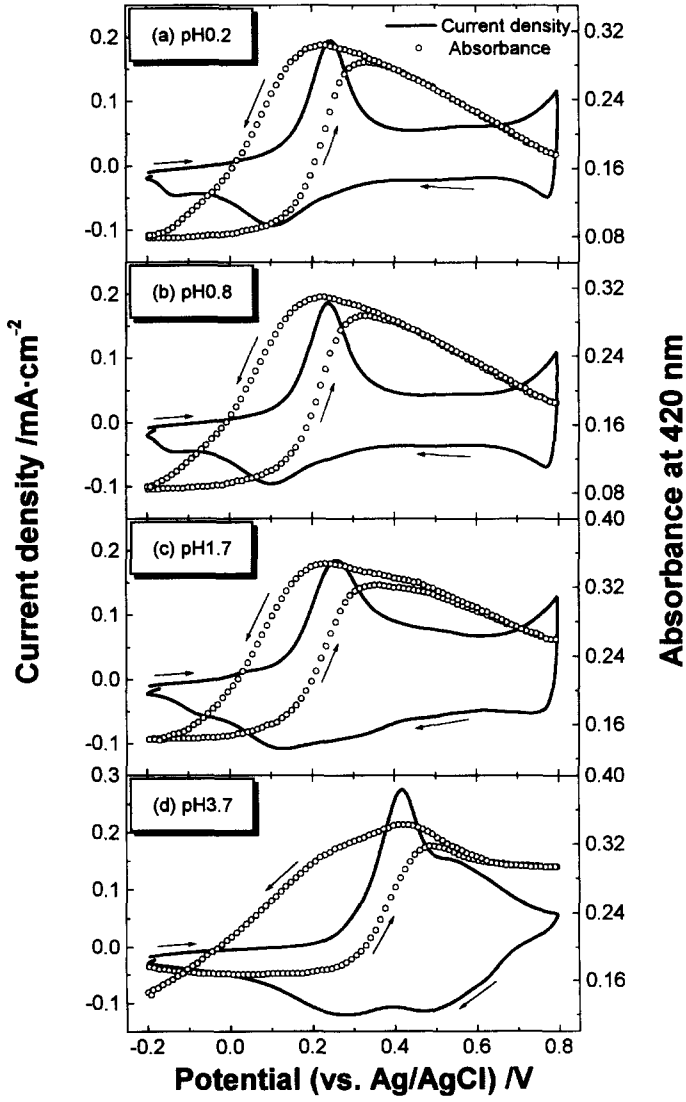

Figure 4 Cyclic voltammograms (solid curves) and absorption responses at 420 nm (circles) of PAn films polymerized at different pH: (a) 0.2; (b) 0.8; (c) 1.7; (d) 3.7. All the measurements were made in 1 M HCl solution

780 cm^{-1} and another weak peak at 930 cm^{-1} that were attributable to out-of-plane bending of C–H bonds of *meta*-substituted aromatic rings[24]. Also a *p*-benzoquinone type peak corresponding to C=O stretching was identified around 1655 cm^{-1}[20,25].

At a first glance we see no such unusual peaks in our spectra, shown in *Figure 5*. However, by careful examination we notice a small shoulder around 1450 cm^{-1} attributable to ν(N–N). Although the spectra of our PAn films have no obvious peak at 1655 cm^{-1} attributable to ν(C=O), we notice that the absorbance at 1655 cm^{-1} is stronger in the film polymerized at pH = 3.7 than that at pH = 0.2. These results may be an indication of the existence of 'head-to-head' heterojunctions and also of an increase in *p*-benzoquinone moieties in the PAn chains obtained at pH = 3.7. We also notice that the relative peak heights are different in the films obtained at different pH: The peaks at 1300 and 1250 cm^{-1} assigned to ν(C–N) (belonging to 'head-to-tail' linkages of anilines) against those at 1500 and 1585 cm^{-1} for ν(C–C) (belonging to phenyl rings in anilines) are lower for the film at high pH than those at low pH. The results imply that the fraction of the 'head-to-tail' junctions in PAn chains is lower in the film obtained at higher pH. Furthermore, the peak assigned to ν(C–N) at around 1300 cm^{-1} shifts depending on the pH at polymerization. This might depend on the length of 'head-to-tail' polymer chains.

u.v.–Vis spectra of PAn films polymerized at different pH

We then observed u.v.–Vis spectra of the PAn films by suspending them in 0.1 M KH_2PO_4 buffer adjusted to different pH but keeping the counter-anion concentration constant at $[Cl^-]$ = 1 M and examined their protonation/deprotonation behaviour through the spectral change upon titration. For comparison the same test was conducted on the same buffered solutions of aniline monomer and two dimers.

Figure 6(a), *Figure 6*(b) show, respectively, spectral changes with pH for aniline monomer and *N*-phenyl-*p*-phenylenediamine ('head-to-tail' dimer). In *Figure 6*(c), *Figure 6*(d) show similar data for two PAn films prepared at pH = 0.2 and 3.7, respectively. For aniline monomer and the head-to-tail dimer the absorption peaks appear in the u.v. region with peak positions being independent of pH of the medium. On the other hand, for the PAn films the absorption spectra are quite different from those of aniline and its dimers and also quite different from each other. We notice that for the PAn film prepared at pH = 3.7 the absorption

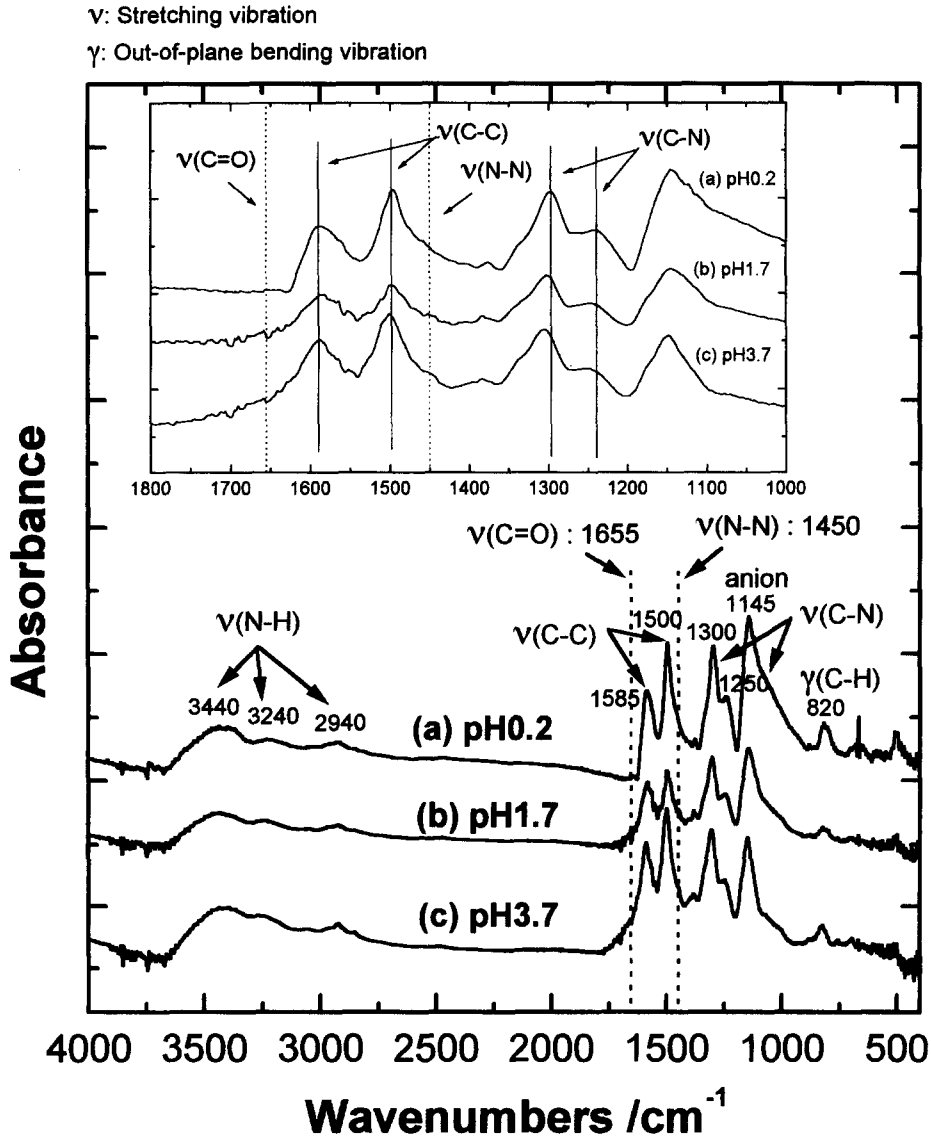

Figure 5 *FTi.r.* spectra of PAn polymerized at (a) pH = 0.2, (b) pH = 1.7 and (c) pH = 3.7

peak shifts by the change of pH of the medium from a high (~12) to a low value (~3) to the visible region of 550 to 800 nm range and for the film prepared at pH = 0.2 to a much longer wavelength region of 600 to over 900 nm range.

Determination of apparent acid dissociation constant

From the spectral changes induced by pH change shown in *Figure 6*, we constructed plots of pH *versus* arbitrarily scaled absorption strengths taken at an arbitrarily chosen wavelength where the dynamic range of the spectral change is the widest (cf. *Figure 6*). The results are shown in *Figure 7*. The pH *versus* absorption strength plot for aniline monomer shows a one-step change, while that of *N*-phenyl-*p*-phenylenediamine (aniline 'head-to-tail' dimer) shows a two-step change, obviously because the former possesses only one primary amino group but the latter a primary and a secondary amino group capable of undergoing protonation/deprotonation at high pH and at low pH, respectively. Although the data are not shown here, that of diphenylamine also exhibited a one-step change, but *p*-benzidine (aniline 'tail-to-tail' dimer) and hydrazobenzene ('head-to-head' dimer) showed a two-step

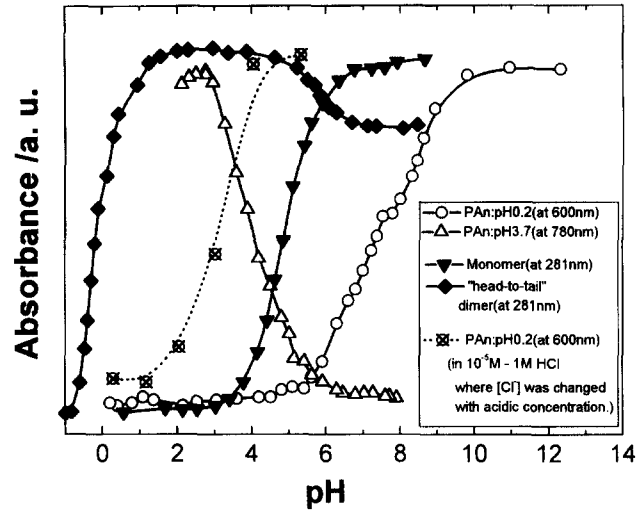

Figure 7 Changes of absorption strength in *Figure 6* of (a) aniline monomer (filled triangles), (b) the 'head-to-tail' dimer (filled squares), (c) PAn films prepared at pH = 0.2 (open circles) and (d) pH = 3.7 (open triangles). The crossed circles show the one measured in 1 M–10^{-5} M HCl solutions for PAn polymerized at pH = 0.2. The absorption strength data were taken at the wavelengths indicated in the figure

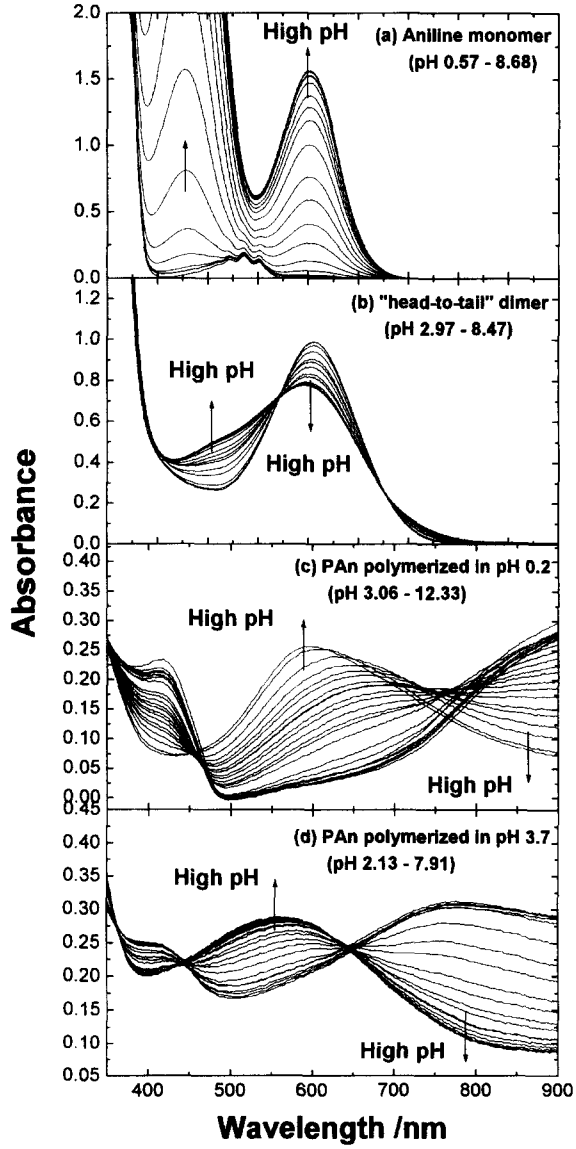

Figure 6 u.v.–Visible spectra in potassium phosphate buffer of (a) 1.12 × 10^{-3} M aniline, (b) 6.29 × 10^{-5} M 'head-to-tail' dimer; (c) PAn films polymerized in pH = 0.2 solution and (d) in pH = 3.7 solution. The range of pH where the spectrum was taken is indicated in each panel

change, reflecting that these latter molecules have two nitrogen atoms on which protonation can take place.

From the absorbance *versus* pH data with equation (3) we determined the *apparent* acid dissociation constant $(pKa)_{app}$. *Figure 8* shows typical examples of $\log\{(Abs_{HAX} - Abs_{obs})/(Abs_{obs} - Abs_A)\}$ *versus* pH plots. The numerical results are summarized in *Table 1* which lists the values of $(pKa)_{app}$ together with the slope m of the $\log\{(Abs_{HAX} - Abs_{obs})/(Abs_{obs} - Abs_A)\}$ *versus* pH plots. For comparison, *Figure 8* also shows the plot (the dotted line) for a PAn film prepared at pH = 0.2 via a *constant potential* mode at + 0.75 V.

The $(pKa)_{app}$ value estimated for aniline is 4.86, which is in good agreement with the literature value of the pKa[23]. The dimers possess two p*K*a values: For the 'head-to-tail' dimer (*N*-phenyl-*p*-phenylenediamine) we determined $(pKa)_{app}$ as 5.72 (= pKa_1) and − 0.1 (= pKa_2), for the 'head-to-head' dimer (hydrazobenzene) as 4.22 (= pKa_1)

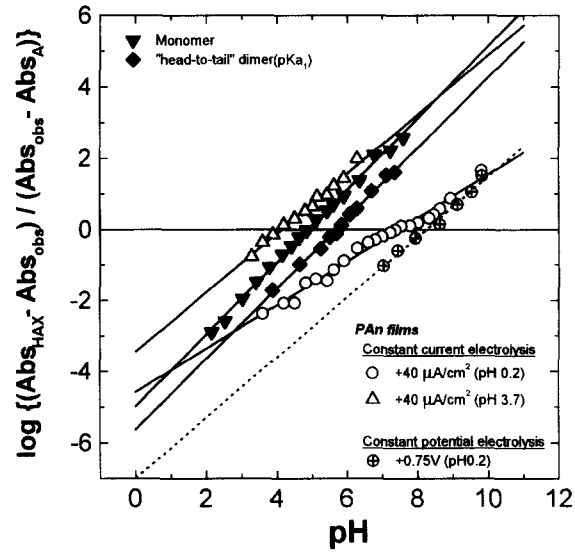

Figure 8 Plots of $\log\{(Abs_{HAX} - Abs_{obs})/(Abs_{obs} - Abs_A)\}$ *versus* pH for aniline monomer filled triangles), the 'head-to-tail' dimer (filled squares) and PAn films polymerized in *constant current* mode at pH = 0.2 (open circles) and 3.7 (open triangles). For comparison, a similar plot for PAn polymerized via a *constant potential* mode (= + 0.75 V) at pH = 0.2 is shown (crossed circles)

and < -1 (= pKa_2), and for the 'tail-to-tail' dimer (*p*-benzidine) as 4.66 (= pKa_1) and 3.57 (= pKa_2). Usually protonation of the second nitrogen occurs only in a strongly acidic solution, except for *p*-benzidine in which the nitrogen atoms are separated by a biphenyl group and thus the protonations can occur in the proximity of 1 pH unit. Anyway, all these values of $(pKa)_{app}$ estimated by equation (3) are in good agreement with the reported values of p*Ka*[23].

For the PAn films, however, we see that the $(pKa)_{app}$ value for the one prepared at low pH (< 1.0) shifts to the high pH side but that for the film prepared at high pH = 3.7 stays below that of the 'head-to-tail' dimer and even below that of aniline (cf. *Table 1*). On $(pKa)_{app}$ of *emeraldine* or conductive form PAn films, entirely different values of $(pKa)_{app}$ evaluated by different methods were reported in the literature[26–29]; this will be discussed in Section 4.

The slope *m* of the $\log\{(Abs_{HAX} - Abs_{obs})/(Abs_{obs} - Abs_A)\}$ *versus* pH plots also gives us a clue to understanding the nature of the primary structure of PAn chains related to the backbone conjugation length. As seen in *Figure 7* the slope *m* for aniline and that for the 'head-to-tail' dimer are close to 1, while that for the PAn film prepared at pH = 3.7 is $\cong$ 0.74 and that for the film prepared at pH = 0.2 is $\cong$ 0.47, which are much smaller than 1. The implication of these results will also be discussed in Section 4.

DISCUSSION

As shown in *Figure 2*, the development of u.v.–Vis spectra of PAn films with polymerization time *t* are different and depend on the pH conditions; this presumably reflects the different primary structure of the PAn chains involved. Although at this point we cannot exactly correlate the u.v.–Vis spectra with the primary structures of the PAn chains, we are certain that the spectra primarily reflect differences in average conjugation length and its distribution along the PAn chains. The spectra of the films prepared at pH = 0.2 suggest that the PAn chains deposited on the WE may have *emeraldine*-type (conductive) backbones with relatively long conjugation length, while those at pH = 3.7 suggest that the PAn chains possess the backbones of relatively short conjugation length interrupted presumably with some heterojunctions and/or unusual bonds.

The results shown in *Figures 3 and 4* imply that deterioration of the PAn chains may take place when the electrolysis potential exceeds a critical value around + 0.8 V. Such a situation is more likely to happen during polymerization at high pH. During the polymerization at low pH (< 1), although the potential exceeds the critical value for a brief period in the very early stage, it subsequently decreases with *t* and stays nearly constant below + 0.8 V. This means that as soon as the polymerization starts the WE surface is covered with conductive *emeraldine* form PAn species and the polymerization potential is reduced, by which means deterioration of the PAn chains can be avoided. On the other hand, for polymerization at higher pH (> 1) the situation is just opposite: increased deposition of insulating species reduces the conductivity of WE and, in turn, increases the potential, further leading to the depolymerization of already existing PAn chains and/or deterioration due to the formation of heterojunctions or other unusual bonds such as *p*-benzoquinone, which is expected to be formed through hydrolysis of the PAn chains[20].

Although, as seen in *Figure 5*, *FT*i.r. spectra on the films prepared at different pH show that the majority of the PAn chains appear to contain *para*-substituted 'head-to-tail' bonds in their backbones, we see traces of N–N bonds corresponding the 'head-to-head' heterojunctions and of C=O bonds corresponding to *p*-benzoquinone moieties in the films prepared at high pH. The relative intensity of the absorbance due to N–N and C=O bonds to that of the C–N bonds corresponding to the 'head-to-tail' junctions is higher for the films obtained at high pH.

As we have seen in *Figure 6*, influences of the pH difference in the polymerization media are also evident in the titration behaviour of the product PAn films, observed by monitoring the change in their u.v.–Vis spectra upon titration. The spectrum of the dimer in *Figure 6*(b) possesses isosbestic points, which suggests that an equilibrium between the protonation/deprotonation states is established upon pH change. The spectrum of the PAn film prepared at pH = 3.7 also possesses isosbestic points, implying that within the PAn chains of relatively short conjugation length an equilibrium between protonation/deprotonation states may also be established. However, the spectra of the film prepared at pH = 0.2 do not exhibit distinct isosbestic points but the peak position shifts steadily to the longer wavelength side with decreasing pH. This implies that the conjugation length increases through the increased protonation of the PAn chains when placed in a low pH medium.

From the titration behaviour of the u.v.–Vis spectra, we were able to estimate $(pKa)_{app}$ or p*Ka** of the PAn films by using equations (3b) and (3c). The results are listed in *Table 1*, which shows that the absorption peak wavelength shifts to the longer wavelength side and p*Ka** is higher for the PAn chains with increasing conjugation length.

Our values of the 'acid dissociation constant' are very different from those reported in the currently available literature for the *emeraldine* form of PAn samples prepared either by oxidative coupling[26,28,29] or by electrochemical polymerization[27] (as employed in this work). The methods employed for determining the 'acid dissociation constant' by these authors[26–29] were based on the fact that the pH-dependence of certain responses of PAn chains such as

Table 1 Apparent acid dissociation constants and other characteristics of PAn films prepared in *constant current* mode with 40 $\mu A\ cm^{-2}$ at different pH, and for aniline and two of its dimers. For comparison, listed are similar data for a PAn film prepared in *constant potential* mode (with 0.75 V, at pH = 0.2)

Acidity of polymerization solutions	The peak wavelengths of protonated/unprotonated species	Apparent acid dissociation constant $(pKa)_{app}$	Slope (*m*) of the plot defied by equation (3)
pH 0.2	975 nm/600 nm	7.45	0.47
pH 0.8	802 nm/589 nm	5.78	0.37
pH 1.7	782 nm/592 nm	5.23	0.61
pH 3.7	775 nm/558 nm	3.98	0.74
pH 0.2 (+ 0.75 V)[a]	876 nm/576 nm	8.32	0.85
Aniline monomer	255 nm/231, 281 nm	4.86	1.01
N-Phenyl-*p*-phenylenediamine	282 nm/280 nm	5.72(pKa_1)	0.99
(Aniline 'head-to-tail' dimer)	256 nm/282 nm	~−0.1(pKa_2)	–
Hydrazobenzene	247 nm/282 nm	4.22(pKa_1)	1.00
Aniline 'head-to-head' dimer	–	< −1(pKa_2)	–

direct current (DC) conductivity and u.v.–Vis absorbance show abrupt change at a certain pH as the result of a dynamic equilibrium between protonated/deprotonated states. For example, MacDiarmid et al.[26] measured the DC conductivity of a PAn pellet recovered from aqueous dispersions of different pH adjusted by varying HCl concentration in the dispersion. They assigned p*Ka** as the pH (≈ 2.5) of the dispersion for which an abrupt change in the DC conductivity of the PAn pellet was observed. Orata and Buttry[27] measured the weight change due to protonation and simultaneous counter-anion doping on PAn chains deposited from H_2SO_4 solutions of different pH on a quartz crystal microbalance (QCM). They assigned p*Ka** ≈ 3 from such a measurement. Wan[28] reported p*Ka** ≈ 3 from u.v.–Vis spectra of a solvent-cast PAn film in aqueous HCl of varying concentration. On the other hand, Stejskal et al.[29] reported p*Ka** ≈ 7 again from u.v.–Vis spectra of PAn dispersion in the media buffered with 0.1 M citric acid and 0.2 M sodium hydrogen phosphate within pH range 2.2–8.0. The first three examples gave p*Ka** ≈ 3, which is much too low and the last p*Ka** ≈ 7 by Stejskal[29] is comparable with our value of $(pKa)_{app} \approx 8$ for electrochemically polymerized PAn film at pH = 0.2.

A conceivable reason for the discrepancy between these two groups is that the former group conducted the determination in unbuffered media with varying counter-anion concentration. Thus their 'apparent acid dissociation constant' is essentially p*Ka** at an unspecified counter-anion concentration defined by equation (3c), while we conducted the determination in well-buffered media with a constant counter-anion concentration of $[Cl^-] = 1$ M so that our p*Ka** $\cong (pKa)_{app}$. These two values of p*Ka** different by $\log[X^-]$. This also applies to the high value of p*Ka** ≈ 7 reported by Stejskal[29]. In fact, we compared equation (3c) and equation (3b) on our PAn film at pH = 0.2 by conducting the titration in unbuffered media with the pH adjusted only by varying the HCl concentration from 10^{-5} to 1 M (pH range 5.3–0.3). The corresponding observed absorbance Abs_{obs} *versus* pH plot is shown in *Figure 7*, from which we determined p*Ka** ≈ 3, as anticipated.

In this connection, the analysis of the acid dissociation behaviour, in particular the slope m of $\log\{(Abs_{HAX} - Abs_{obs})/(Abs_{obs} - Abs_A)\}$ *versus* pH plots also provides us an interesting clue to understanding the structure of PAn chains prepared at different pH (again when the titration was conducted in a medium at a constant counter-anion concentration or ionic strength).

As seen in *Figure 8* and *Table 1*, the slope m of the plots for aniline and its dimers are close to 1, while those for PAn films are much less than 1. If the protonation proceeds as a single-site process as defined in equations (1) and (2), the slope m must be 1. Even if a system possesses multiple sites but the protonation occurs at each site independent of the neighbouring sites, again the slope m should be 1 and $(pKa)_{app}$ agrees with p*Ka*. In such a system the spectral changes should occur intensively around pH = p*Ka* with isosbestic points, if they exist, such as we have seen in *Figure 6*. This behaviour is probably due to the polydispersity in the conjugation lengths of the *para*-substituted sequences. If the distribution is broad, we should observe gradual change in the absorbance and thus the slope $m < 1.0$, because the chains involved should have different absorption strength and different acid dissociation constant at the given wavelength.

Thus the values of $(pKa)_{app}$ or p*Ka** (although these two are different by $\log[X^-]$) and the slope m of the $\log\{(Abs_{HAX} - Abs_{obs})/(Abs_{obs} - Abs_A)$ *versus* pH plots are a good measure reflecting the characteristics of the conjugated backbone structure of the PAn chains: the larger value of $(pKa)_{app}$ the longer the average conjugation length, while the smaller the value of the slope m, the broader the distribution and/or the larger the heterogeneity in the conjugation lengths of the PAn backbones.

In connection to this issue, for the films prepared at pH = 0.2 and 0.8 we see little difference in their voltammograms and u.v.–Vis spectra, but nevertheless the $(pKa)_{app}$, and the slope m are considerably different, indicating their conjugation backbone structures are different. It is worthwhile noting that for the PAn film prepared under a *constant potential* mode of + 0.75 V at pH = 0.2, under which undesirable degradation of PAn chains could have been avoided, the value of $(pKa)_{app}$ is larger, while the slope m is closer to 1, implying their PAn chains are of longer average length and are more homogeneous in their conjugated backbone structure.

CONCLUSIONS

(1) The features of $(pKa)_{app}$ and the u.v.–Vis spectra of PAn chains compared with those of aniline and its dimers suggest that the PAn chains assume the *emeraldine* form, and that the protonation of their imino groups is stabilized by the resonance structure.

(2) The $(pKa)_{app}$ and the slope m of $\log\{(Abs_{HAX} - Abs_{obs})/(Abs_{obs} - Abs_A)$ *versus* pH plots reflect the average conjugation length and the polydispersity of the conjugated structure of the PAn backbones.

(3) The $(pKa)_{app}$, became more alkaline and m became smaller when the polymerization was carried out in low pH solutions. This means that the PAn chains polymerized in low pH solution have a longer conjugation length in their backbones but greater polydispersity.

(4) To obtain PAn chains with a longer average conjugation length and a narrower distribution via electrochemical polymerization, we should avoid as much as possible the situation under which the electrolysis potential exceeds + 0.8 V, although we do not know yet that the performance of such PAn films are, in fact, better or not than the PAn films prepared otherwise.

REFERENCES

1. Osaka, T., Ogano, S., Naoi, K. and Oyama, N., *J. Electrochem. Soc.*, 1989, **136**, 306.
2. Yonezawa, S., Kanamura, K. and Takehara, Z., *J. Electrochem. Soc.*, 1989, **140**, 629.
3. Kobayashi, T., Yoneyama, H. and Tamura, H., *J. Electroanal. Chem.*, 1984, **161**, 419.
4. Jelle, B. P. and Hagen, G., *J. Electrochem. Soc.*, 1993, **140**, 3560.
5. Genies, E. M., Boyle, A., Lapkowski, M. and Tsintavis, C., *Polyaniline: A Historical Survey. Synthetic Metals*, 1990, **36**, 139.
6. Genies, E. M. and Tsintavis, C., *J. Electroanal. Chem.*, 1985, **195**, 109.
7. Genies, E. M. and Lapkowski, M., *J. Electroanal. Chem.*, 1987, **220**, 67.
8. McManus, P. M., Cushman, R. J. and Cheng Yang, S., *J. Phys. Chem.*, 1987, **91**, 744.
9. Huang, W., Humphrey, B. D. and MacDiarmid, A. G., *J. Chem. Soc., Faraday Trans. 1*, 1986, **82**, 2385.
10. Osaka, T., Nakajima, T., Naoi, K. and Owens, B. B., *J. Electrochem. Soc.*, 1990, **137**, 2139.

11. Yang, H. and Bard, A. J., *J. Electroanal. Chem.*, 1992, **339**, 423.
12. Shim, Y., Won, M. and Park, S., *J. Electrochem. Soc.*, 1990, **137**, 538.
13. Bade, K., Tsakova, V. and Schultze, J. W., *Electrochimica Acta*, 1992, **37**, 2255.
14. Córdova, R., del Valle, M. A., Arratia, A., Gómez, H. and Schrebler, R., *J. Electroanal. Chem.*, 1990, **377**, 75.
15. Scharifker, B. R. and Mostany, J., *J. Electroanal. Chem.*, 1984, **177**, 13.
16. Scharifker, B. and Hills, G., *Electrochemical Acta*, 1983, **28**, 879.
17. Brett, C. M. A. and Brett, A. M. O. *Electrochemistry; Principles, Methods and Applications*. Oxford, 1994, p. 341.
18. Lide, D. R., ed. *CRC Handbook of Chemistry and Physics*, 76th edn, CRC Press, 1995–1996, p. p5-95.
19. Shim, Y., Won, M. and Park, S., *J. Electrochem. Soc.*, 1990, **137**, 538.
20. Seeger, D., Kowalchyk, W. and Korzeniewski, C., *Langmuir*, 1990, **6**, 1527.
21. Aoki, K., Cao, J. and Hoshino, Y., *Electrochimica Acta*, 1994, **39**, 2291.
22. Koziel, K., Lapkowski, M. and Lefrant, S., *Synthetic Metals*, 1995, **69**, 217.
23. Lide, D. R., ed. *CRC Handbook of Chemistry and Physics*, 76th edn. CRC Press, 1995–1996, pp. p8-43-p8-55.
24. Ohsaka, T., Ohnuki, Y., Oyama, N., Katagiri, G. and Kamisako, K., *J. Electroanal. Chem.*, 1984, **161**, 399.
25. Silverstein, R. M., Bassler, G. C. and Morrill, T. C. *Spectrometric Identification of Organic Compounds*. Wiley, Chichester, 1991.
26. Chiang, J. and MacDiarmid, A. G., *Synthetic Metals*, 1986, **13**, 193.
27. Orata, D. and Buttry, D. A., *J. Am. Chem. Soc.*, 1987, **109**, 3574.
28. Wan, M., *J. Polym. Sci., Polym. Chem.*, 1992, **30**, 543.
29. Stejskal, J., Kratochvíl, P. and Radhakrishnan, N., *Synthetic Metals*, 1993, **61**, 225.